Received: 18 September 2018 | Accepted: 15 November 2018

DOI: 10.1002/jcp.27883

ORIGINAL RESEARCH ARTICLE

WILEY Journal of Cellular Physiology

27-Hydroxycholesterol enhanced osteoclastogenesis in lung adenocarcinoma microenvironment

Lishan Zhang[2] | Ming Liu[3] | Jinglei Liu[4] | Xingkai Li[5] | Ming Yang[6] | Benhua Su[7] | Yanliang Lin[1]

[1]Department of Center Laboratory, Shandong Provincial Hospital Affiliated to Shandong University, Jinan, China

[2]Department of Hand and Foot Surgery, Shandong Provincial Hospital Affiliated to Shandong University, China

[3]Department of Cardiothoracic Surgery, Gansu Provincial Hospital of TCM, Lanzhou, Jinan, China

[4]Department of Gastrointestinal Surgery, Shandong Provincial Hospital Affiliated to Shandong University, Jinan, China

[5]Department of Thoracic Surgery, Shandong Provincial Hospital Affiliated to Shandong University, Jinan, China

[6]Department of Ultrasound, Shandong Provincial Hospital Affiliated to Shandong University, Jinan, China

[7]Department of Medical Engineering, Shandong Provincial Hospital Affiliated to Shandong University, Jinan, China

Correspondence
Yanliang Lin, Department of Center Laboratory, Shandong Provincial Hospital Affiliated to Shandong University, 544 Jingsi Road, Jinan 250021, PR China.
Email: sphyanlianglin@163.com
Benhua Su, Department of Medical Engineering, Shandong Provincial Hospital Affiliated to Shandong University, 324 Jingwu Road, Jinan 250021, PR China.
Email: sbh1025@163.com

Funding information
National Natural Science Foundation of China, Grant/Award Numbers: 81572272, 81201778; Medical and Health Technology Development Plan Project of Shandong Province, Grant/Award Number: 2016WSB01041; Science and Technology Development Plan Project of Shandong Province, Grant/Award Number: 2015 GSF118083

Abstract

27-Hydroxycholesterol (27-HC) has been implicated in the pathological process of estrogen receptor positive breast cancer. However, the role of 27-HC in lung adenocarcinoma is still unclear. Because bone metastasis is a main reason for the high mortality of lung adenocarcinoma, this study aimed to investigate the effect of 27-HC on osteoclastogenesis in lung adenocarcinoma microenvironment. The results showed that the conditioned media (CM) from lung adenocarcinoma cells cocultured with macrophages promoted osteoclast differentiation, which was enhanced by 27-HC. Further investigation showed that CM inhibited miR-139 expression and promoted c-Fos expression. Luciferase reporter assay identified c-Fos as a direct target of miR-139. CM also induced the expression and nuclear translocation of NFATc1 and STAT3 phosphorylation, which was enlarged by 27-HC but was attenuated by miR-139. Coimmunoprecipitation assay demonstrated that 27-HC increased the interaction between NFATc1 and phosphorylated STAT3, which was restricted by miR-139. Chromatin immunoprecipitation assay showed that pSTAT3 could bind to the promoter of c-Fos, c-Fos could bind to the promoter of NFATc1, and both pSTAT3 and NFATc1 could bind to the promoter of Oscar, which were enlarged by 27-HC but were blocked by miR-139. Knockdown of c-Fos mimicked the effect of miR-139. These results suggested that CM, especially containing 27-HC, promoted osteoclastogenesis by inhibiting miR-139 expression and activating the STAT3/c-Fos/NFATc1 pathway.

KEYWORDS
c-Fos, miR-139, NFATc1, osteoclast, 27-hydroxycholesterol

1 | INTRODUCTION

Osteolytic bone metastasis is a frequent event in the late stage of lung cancer (Luis-Ravelo et al., 2014). Metastatic tumor cells can affect bone remodeling by regulating the interaction with osteoblasts and osteoclasts (Coughlin et al., 2017). After tumor cells spread to bone tissue, several cell types are recruited into the microenvironment that supports the cytokines secretion, immune responses, osteoblast, and osteoclast differentiation (Bussard, Gay, & Mastro, 2008). The immune cells may play key roles in communication between tumor cells and skeletal functional cells (Bussard et al., 2008). Tumor cells can interact with immune cells to secrete some cytokines, which in turn stimulates osteoclast differentiation.

Osteoclasts are a kind of multinucleated giant cells that regulate bone resorption (Pereira et al., 2018). Osteoclast differentiation requires two critical factors, macrophage-colony stimulating factor (M-CSF) and receptor activator of nuclear factor κB ligand (RANKL; Koga et al., 2005). These molecules can be produced by osteoblasts, immune cells, and fibroblasts (Wythe, Nicolaidou, & Horwood, 2014). Tumor cells also secrete a variety of cytokines for osteoclast differentiation, including PTHrP, IL-1β, IL-6, IL-8, TGF-β1, GM-CSF, M-CSF, and TNF-α (Hernandez, Moreno, Zandueta, Montuenga, & Lecanda, 2010; Kuo, Liao, Hung, Huang, & Hsu, 2013; B. K. Park et al., 2007; Schulze et al., 2012; Shih, Shih, & Chen, 2004; Yamada et al., 2016), among of which some factors stimulate the expression of RANKL in osteoblast and promote osteoclast differentiation (Kuo et al., 2013). A series of transcriptional factors are implicated in osteoclast differentiation, such as NFATc1, c-Fos, and PU.1 (S. Y. Park et al., 2015). RANKL stimulates the expression of activator protein 1 (AP-1) composed of Fos and Jun (Hyeon, Lee, Yang, & Jeong, 2013). During osteoclast differentiation, c-Fos plays a key role in expression and nuclear translocation of NFATc1 (M. Asagiri & Takayanagi, 2007). NFATc1 acts as a partner of AP-1 to recognize the promoters of multiple targeted genes involved in osteoclastogenesis, including tartrate-resistant acid phosphatase (TRAP) and cathepsin K (M. Asagiri & Takayanagi, 2007). Tumor cell-derived cytokines might regulate the expression of NFATc1 and c-Fos in osteoclast precursors in bone marrow microenvironment.

27-Hydroxycholesterol (27-HC) is the most prevalent circulating oxidized cholesterol and is particularly abundant in atherosclerotic plaques (Carpenter et al., 1995). 27-HC can trigger the secretion of tumor necrosis factor-α (TNFα) and interleukin-8 (IL-8) from macrophages (S. M. Kim et al., 2013; Koarai et al., 2012). TNF-α has been identified as an effective inducer of osteoclast differentiation (Courbon et al., 2017). IL-8 can stimulate osteoclastogenesis independent of the RANKL pathway (Bendre et al., 2005). Thus, we hypothesized that 27-HC could enhance osteoclastogenesis in the coculture system of lung adenocarcinoma cells and macrophage. In the present study, we set out to investigate the role of 27-HC in osteoclast differentiation in lung adenocarcinoma microenvironment.

2 | MATERIALS AND METHODS

2.1 | Materials

27-HC was purchased from Yuanye Biological Technology (Shanghai, China); a Leukocyte Acid Phosphatase Kit was purchased from Sigma (St. Louis, MO); Dulbecco's modified Eagle's medium (DMEM) medium and fetal bovine serum (FBS) were purchased from Invitrogen Life Technologies (Grand Island, NY); anti-NFATc1, anti-c-Fos, and anti-β-actin were purchased from Abcam (Cambridge, MA); anti-STAT3 and anti-pSTAT3 were purchased from Cell Signaling Technology (Beverly, MA).The rabbit anti-goat secondary antibody (BA1060) was purchased from Boster. The goat anti-rabbit secondary antibody (ZB-2301) was purchased from ZSGB-Bio (Beijing, China).

2.2 | Cell culture

The lung adenocarcinoma cells A549 and NCI-H1299 were cultured in DMEM supplemented with 10% FBS, 100 IU/ml penicillin and 100 mg/ml streptomycin at 37°C in a humidified atmosphere of 5% CO_2. THP-1 cells were cultured in DMEM with 10% FBS, penicillin/streptomycin, and 100 ng phorbol-12-myristate-13-acetate (PMA) for 48 hr. To exclude the effect of PMA, THP-1-derived macrophages were cultured in DMEM with 10% FBS for another 24 hr. In Transwell chamber, THP-1-derived macrophages were grown in the low chamber containing DMEM with 10% FBS and antibiotics in the presence or absence of 27-HC and A549, and NCL-H1299 cells were seeded into the upper chambers containing free-serum DMEM. After 24 hr of culture, the supernatant was collected and passed through 0.2-μM filter to use for conditioned media (CM). For osteoclast differentiation, RAW264.7 cells were plated into 24-well plate at a density of 2×10^4, and were cultured in CM for 6 days. The media were replaced by fresh CM daily.

2.3 | Tartrate-resistant acid phosphatase staining

Cells were fixed with 4% paraformaldehyde and stained for TRAP using a Leukocyte Acid Phosphatase Kit (Sigma). TRAP-positive cells containing three or more nuclei were considered as multinucleated osteoclasts. The cell fusion index was calculated according to the method previously described by us.

2.4 | Protein extraction and western blot analysis

The total protein was isolated using RIPA lysis buffer (Thermo Fisher Scientific, Waltham, MA). The cytoplasmic protein and nuclear protein were isolated according to the method previously described (Ma et al., 2016). The protein concentration was measured by the bicinchoninic acid method. Equal amounts of proteins were subjected to sodium dodecyl sulfate polyacrylamide gel electrophoresis, followed by electrotransfer to polyvinylidene difluoride membranes. The membranes were blocked for 1 hr with 5% nonfat milk, and were then labelled with primary antibodies

including anti-β-actin (1:2000), anti-c-Fos (1:1000), anti-NFATc1 (1:500), anti-STAT3 (1:2000), and anti-pSTAT3 (Tyr705, 1:1000). After washed using TBST, the membranes were incubated with horseradish peroxidase-conjugated secondary antibodies for 1 hr at room temperature. The protein bands were visualized using the enhanced chemiluminescence method.

2.5 | RNA extraction and northern blot analysis

Total RNA was extracted using TRIzol reagent (Invitrogen, Carlsbad, CA). Northern blot analysis was performed as previously described. Thirty micrograms of RNA was loaded onto a 15% urea–polyacrylamide gel, followed by electrotransfer to nylon membrane using Trans-blot cell (Bio-Rad, Hercules, CA). The expression of miR-139-5p or U6 was detected using biotin-labeled oligonucleotide probes (5′-ACTCCAA CAGGGCCGCGTCTCCA-3′ for mmu-miR-139-5p; 5′-TATTCTTATAT TTTCTGTGACAT-3′ for U6).

2.6 | Quantitative reverse transcription polymerase chain reaction

The complementary DNA (cDNA) was obtained by reverse transcription using the RevertAid First Strand cDNA Synthesis Kit (Fermentas). The cDNA was used as template to amplify c-Fos with the specific primers (forward, 5′-TGTTCTCGGGTTTCAACG-3′ and reverse, 5′-TTATCCCT TCGGCATCAC-3′), and GADPH with the primers (forward, 5′-GGATG CTGCCCTTACCC-3′ and reverse, 5′-CCTCCCGCCCTGCTTAT-3′). The expression of miR-139-5p was measured using the TeqMan MicroRNA assay Kit (ABI, Foster City, CA) in the LightCycler 480 system (Roche). The small nuclear RNA U6 was used for a normalizing control. The miR-139-5p expression was evaluated using the comparative cycle threshold value. Each sample was performed in triplicate.

2.7 | Luciferase reporter assay

The sequence containing murine miR-139 targeting site at position 537–543 of c-Fos 3′UTR were amplified using forward (5′-TCCAATTA GAAACGACCAA-3′) and reverse (5′-TCAGAACATTCAGACCACC-3′) primers. The PCR product was cloned into pMIR-REPORT (Promega, Madison). HEK293 cells were cotransfected with 200 ng reporter vector, 30 nM wild-type miR-139 or mutant miR-139 using Lipofectamine 3000, and 5 ng pRL-SV40 plasmid (Promega). After 24-hr of incubation, luciferase activities were measured using the Dual-Luciferase Assay (Promega) according to the manufacturer's instructions.

2.8 | Gene transfection

Raw264.7 cells were seeded at a density of 2×10^4 cells/ml in 24-well microplates overnight. The cells were then transfected with small interfering RNA against c-Fos, miR-139 or anti-miR-139 (Biosune, Shanghai, China) using Lipofectamine 3000 (Invitrogen) for 6 hr. After the media was replaced by fresh complete DMEM medium, cells were cultured for 48 hr.

2.9 | Coimmunoprecipitation assay and chromatin immunoprecipitation assay

Immunoprecipitation was performed as described previously (Zhang, Lv, Xian, & Lin, 2017). In brief, cells were incubated for 30 min in a cold lysis buffer (20 mM Tris [pH 7.5], 150 mM NaCl, 1 mM ethylenediaminetetraacetic acid, 1 mM egtazic acid, 1% Triton X-100, 2.5 mM sodium pyrophosphate, 1 mM β-glycerophosphate,1 mM Na_3VO_4 and phenylmethylsulfonyl fluoride, 1 mg/ml leupeptin). The lysates were obtained by centrifugation and incubated with indicated antibodies and Protein G-Sepharose (Invitrogen, Life Technologies, Carlsbad, CA) at 4°C for 2 hr, and was analyzed by western blot.

Chromatin immunoprecipitation assay (ChIP) was performed as described previously (Zhang et al., 2017). Briefly, treated cells were cross-linked using fresh 1% formaldehyde for 10 min at room temperature. Unreacted formaldehyde was quenched using glycine. The cells were harvested and resuspended in sodium dodecyl sulfate lysis buffer. After centrifugation, the cell lysates were obtained and sonicated to share DNA to 200–1,000 base pairs in length. Protein/DNA complexes were precipitated using indicated antibodies or control immunoglobulin G. After crosslinks were reversed using NaCl, free DNA was purified using spin columns, and was subjected to PCR amplification using specific primers (forward primer, 5′-TCTCAGGTCCCAGACGCCAAAA-3′ and reverse primer, 5′-GCAGCCTGGAAACTGCGCTTA-3′ to identify the binding site of pSTAT3 on c-Fos promoter; forward primer, 5′-GGGACGC CCATGCAATCTGTTAGTA-3′ and reverse primer, 5′-GCTGAAGTCATTA TGTAAAATCGCAGGCT-3′ to identify the binding site of c-Fos on NFATc1 promoter; forward primer, 5′-TAGACATAAGCTCATTCTGGAA AT-3′ and reverse primer, 5′-GCTCAATCGGAGATGGGTAG-3′ to identify the binding site of pSTAT3 on Oscar promoter; forward primer, 5′-TTTGTTGTTGTTGTTGTTTT-3′ and reverse primer, 5′-GTCATAGTTT CATTGTCTTGG-3′ to identify the binding site of NFATc1 on Oscar promoter).

2.10 | Immunofluorescence

Cells were fixed with 4% paraformaldehyde for 10 min, permeabilized with 0.2% Triton X-100 for 5 min, and blocked with 2% bovine serum albumin for 1 hr at room temperature. After rinsing with PBST, cells were labelled with anti-NFATc1 (1:500) or anti-pSTAT3 (1:100) overnight at 4°C. Then, the cells were incubated with Texas Red-conjugated or fluorescein isothiocyanate-conjugated secondary antibodies for 1 hr, respectively. Cell images were captured using confocal laser scanning microscopy (Leica, Wetzlar, Germany).

2.11 | Statistical analysis

Statistical analysis was performed using GraphPad Prism 5.0 (GraphPad Software, San Diego, CA). All data are presented as mean ± standard deviation from at least three independent experiments. Student's *t* test was used to determine the difference between two groups. One-way analysis of variance was used to determine the difference among multiple groups. $p < 0.05$ was considered as statistical significance.

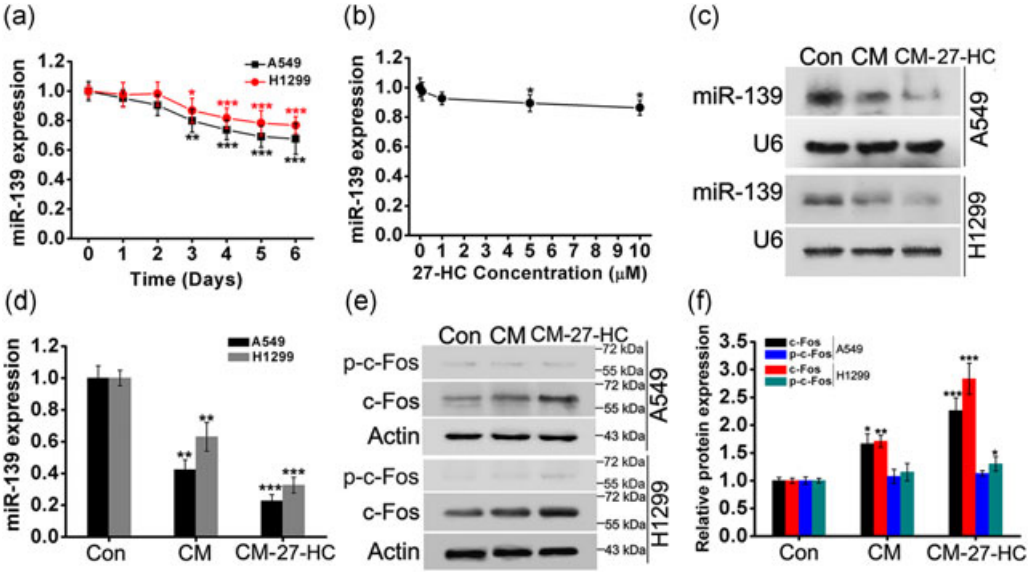

FIGURE 1 27-HC enhanced the effect of conditioned media (CM) on expression of miR-139-5p and c-Fos. The RAW264.7 cells were cultured in the CM from coculture system of A549 or H1299 cells and THP-1-derived macrophages for 6 days. To determine the effect of 27-hydroxycholesterol (27-HC), the RAW264.7 cells were treated with different concentration of 27-HC for 6 days. (a) The time curve of miR-139 expression in RAW264.7 cells treated with CM. (b) The effect of 27-HC on miR-139 expression in RAW264.7 cells. (c) The RAW264.7 cells were cultured in CM in the presence or absence of 5 μM 27-HC for 6 days. The expression of miR-139-5p was determined by northern blot analysis. (d) The RAW264.7 cells were cultured in CM in the presence or absence of 5 μM 27-HC for 6 days. RT-PCR was used to determine miR-139-5p expression. (e) The RAW264.7 cells were cultured in CM in the presence or absence of 5 μM 27-HC for 6 days. The expression and phosphorylation of c-Fos was measured by western blot analysis. (f) The RAW264.7 cells were cultured in CM in the presence or absence of 5 μM 27-HC for 6 days. RT-PCR was used to determine the mRNA expression of c-Fos. Data represent means ± *SD* of at least three independent experiments. $^{*}p < 0.05$; $^{**}p < 0.01$; $^{***}p < 0.001$. 27-HC: 27-hydroxycholesterol; mRNA: messenger RNA; RT-PCR: reverse transcription polymerase chain reaction; *SD*: standard deviation [Color figure can be viewed at wileyonlinelibrary.com]

3 | RESULTS

3.1 | CM from lung adenocarcinoma cells cocultured with THP-1-derived macrophage inhibited miR-139 expression and promoted c-Fos expression in RAW264.7 cells

When they spread to bone tissues, tumor cells can stimulate osteoblasts to secrete M-CSF and RANKL for osteoclast differentiation, which in turn accelerates tumor bone metastases (Thomas et al., 1999). Given that macrophages play key roles in tumor metastases, we speculated that the interaction between tumor cells and macrophages affected osteoclast-related genes expression during osteoclast differentiation. In this study, we found that CM from A549 or H1299 cells cocultured with THP-1-derived macrophage inhibited miR-139 expression in osteoclast precursor RAW264.7 cells in a time-dependent manner (Figure 1 a). Exposure of RAW264.7 cells to 5 and 10 μM 27-HC also reduced the miR-139 level (Figure 1b). Northern blot analysis confirmed that miR-139 expression was inhibited in RAW264.7 cells cultured in CM for 6 days (Figure 1c,d). We further tested the effect of 27-HC-treated CM on the expression of miR-139. The results showed that miR-139 expression was lower in RAW264.7 cultured in CM containing 5 μM 27-HC for 6 days compared with CM group (Figure 1c,d). Further investigation showed that exposure of RAW264.7 cells to CM promoted the expression of c-Fos, which was enhanced by 27-HC (Figure 1e,f). The results indicated that 27-HC enlarged the inhibitory effect of CM on miR-139 expression and the stimulating effect of CM on c-Fos expression.

3.2 | c-Fos was identified as a direct target of miR-139

We further explored the relation between miR-139 and c-Fos. As shown in Figure 2a, one putative recognition site for murine miR-139 was found in the 3′UTR of c-Fos by TargetScan (http://www.targetscan.org/). The sequence containing this site were cloned into the luciferase reporter vector to construct a plasmid carrying c-Fos 3′UTR (pMIR-c-Fos). 293 T cells were cotransfected with pMIR-c-Fos and miR-139-WT (wild-type) or miR-139-MT (mutant type). The results showed that miR-139-WT notably reduced luciferase activities whereas miR-139-MT slight increased luciferase activities (Figure 2b). Further investigation demonstrated that miR-139 overexpression not only inhibited the protein expression and phosphorylation of c-Fos, but also reduced the messenger RNA (mRNA) expression of c-Fos (Figure 2c,d). In contrast, anti-miR-139 overexpression promoted the protein and mRNA expression of c-Fos, but did not significantly affect the phosphorylation of c-Fos (Figure 2c,d). These results suggested that c-Fos was a direct target of miR-139.

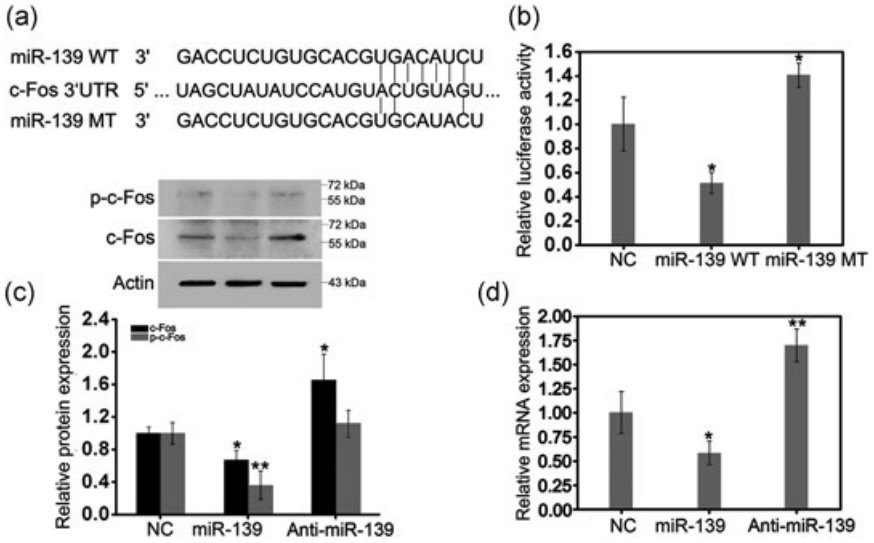

FIGURE 2 c-Fos was a direct target of miR-139. (a) The putative miR-139 targeted site in the 3′UTR region of c-Fos. (b) HEK293 cells were transfected with wild-type miR-139 (miR-139 WT) or mutant miR-139 (miR-139 MT) and c-Fos-3′UTR. The luciferase activities were measured by the Dual-Luciferase Assay; $^{*}p < 0.05$. (c) The RAW264.7 cells were transfected with miR-139 or anti-miR-139. Western blot analysis was used to determine the protein expression and phosphorylation of c-Fos; $^{*}p < 0.05$. (d) RT-PCR was used to determine the mRNA expression of c-Fos; $^{*}p < 0.05$, $^{**}p < 0.01$. mRNA: messenger RNA; NC: negative control; RT-PCR: reverse transcription polymerase chain reaction

3.3 | miR-139 reversed CM-induced the expression and nuclear translocation of NFATc1, phosphorylation of STAT3 and interaction between phosphorylated STAT3 and NFATc1

To explore the mechanism of how miR-139 regulated osteoclast differentiation, we tested the effect of miR-139 on the expression of NFATc1. Our results showed that CM from the coculture system of A549 or H1299 cells and THP-1-derived macrophages-induced NFATc1 expression in RAW264.7 cells, which was enhanced by 27-HC (Figure 3a). Overexpression of miR-139 inhibited-NFATc1 expression induced by CM despite the presence of 27-HC (Figure 3a). Meanwhile, 27-HC enhanced CM-induced phosphorylation of STAT3, which was significantly inhibited by miR-139 overexpression (Figure 3b). 27-HC treatment increased the nuclear NFATc1 and reduced the cytoplasmic NFATc1, suggesting that 27-HC-induced nuclear translocation of NTATc1, which was blocked by miR-139 (Figure 3c). Immunofluorescence staining showed that 27-HC augmented CM-induced nuclear translocation of NFATc1 and phosphorylation of STAT3 (Figure 3d). Coimmunoprecipitation assay demonstrated that 27-HC treatment increased the interaction between phosphorylated STAT3 (pSTAT3) and NFATc1, which was attenuated by miR-139 (Figure 3e). These results indicated that miR-139 inhibited CM induced the expression and nuclear translocation of NFATc1, phosphorylation of STAT3 and interaction between pSTAT3 and NFATc1, regardless of the presence of 27-HC. To determine the transcriptional regulation among STAT3, NFATc1, and c-Fos ChIP assay was performed. The results showed that exposure of RAW264.7 cells to CM induced the recruitment of pSTAT3 to the promoter of c-Fos, which was strengthened by 27-HC (Figure 3f). 27-HC also enhanced CM induced the binding of c-Fos to the promoter of NFATc1 (Figure 3f). In addition, 27-HC promoted the recruitment of pSTAT3 and NFATc1 to the promoter of Oscar (Figure 3f). These results suggested that pSTAT3 directly regulated the transcription of c-Fos, c-Fos mediated the transcription of NFATc1, and then pSTAT3 cooperated withNFATc1 to control the transcription of Oscar.

3.4 | Knockdown of c-Fos inhibited CM-induced osteoclast differentiation

To verify the role of c-Fos in molecular regulation during osteoclast differentiation, knockdown of c-Fos was performed. RAW264.7 cells and c-Fos-depleting cells were cultured in CM containing 27-HC for 48 hr. As shown in Figure 4a, in RAW264.7 cells, the expression of pSTAT3 reached the peak at 12 hr and returned to baseline at 48 hr. The expression and phosphorylation of c-Fos were induced to the maximum level at 12 hr, and was then gradually reduced at 24 and 48 hr. The expression of NFATc1 and Oscar were progressively increased within 48 hr. These results suggested that exposure of RAW264.7 cells to CM with 27-HC first induced phosphorylation of STAT3, and next pSTAT3 positively regulated c-Fos expression, and then c-Fos promoted NFATc1 expression, and finally NFATc1 cooperated with pSTAT3 to regulate Oscar expression, which was consistent with the results of ChIP assay (Figure 3f). Contrastingly, c-Fos-knockdown blocked the expression of pSTAT3, NFATc1 and Oscar (Figure 4a). Inhibition of c-Fos also blocked the interaction between pSTAT3 and NFATc1 (Figure 4b), which was similar to the effect of miR-139 (Figure 3e). Following the above findings, we tested the roles of miR-139 and c-Fos in osteoclast differentiation from RAW264.7 cells cultured in CM containing 27-HC for 6 days. The results showed that exposure of RAW264.7 cells to CM with 27-HC-induced dose-dependent osteoclast

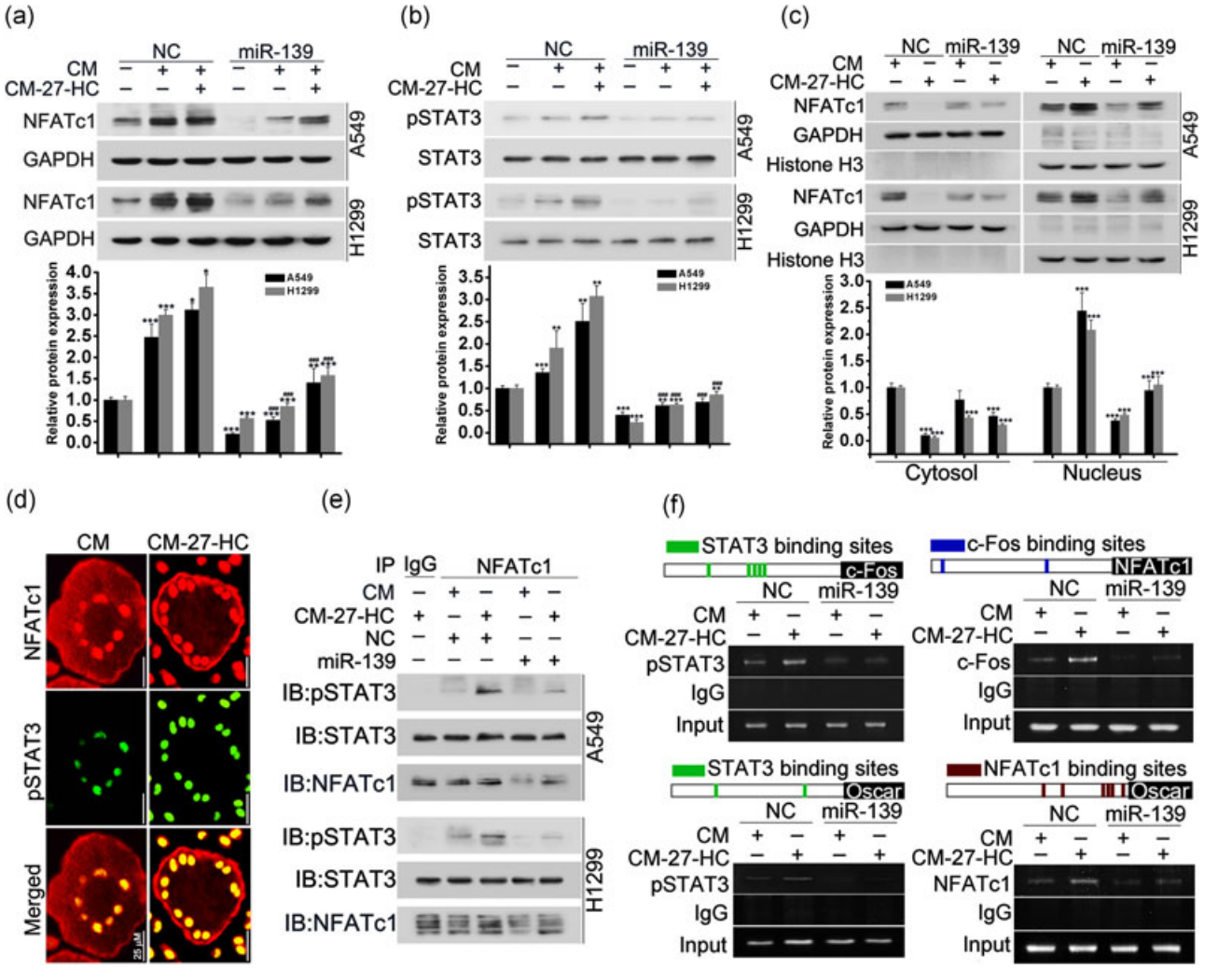

FIGURE 3 miR-139 suppressed CM induced the expression and nuclear translocation of NFATc1 and phosphorylation of STAT3. The RAW264.7 cells were transfected with negative control (NC) or miR-139, and were cultured in CM in the presence or absence of 27-HC. (a) miR-139 inhibited CM-induced NFATc1 despite the presence of 27-HC. $^{*}p < 0.05$ versus CM group; $^{**}p < 0.01$ versus CM group; $^{***}p < 0.001$ versus CM group; $^{\#\#\#}p < 0.001$ versus the corresponding NC group. (b) miR-139 suppressed CM-induced phosphorylation of STAT3 despite the presence of 27-HC. $^{**}p < 0.01$ versus CM group; $^{***}p < 0.001$ versus CM group; $^{\#\#\#}p < 0.001$ versus the corresponding NC group. (c) miR-139 suppressed CM-induced nuclear translocation of NFATc1 despite the presence of 27-HC. $^{***}p < 0.001$ versus CM group. (d) The expression of NFATc1 and pSTAT3 were determined by immunofluorescence staining. (e) miR-139 blocked CM induced the interaction between NFATc1 and phosphorylated STAT3. $^{*}p < 0.05$ versus CM group; $^{**}p < 0.01$ versus CM group; $^{***}p < 0.001$ versus CM group; $^{\#\#\#}p < 0.001$ versus the corresponding NC group. (e) The binding capacity of pSTAT3 the promoters of c-Fos and Oscar, the binding capacity of c-Fos to the promoter of NFATc1 and the binding capacity of NFATc1 to the promoter of Oscar were determined by ChIP assay, respectively. 27-HC: 27-hydroxycholesterol; CM: conditioned media; GAPDH: glyceraldehyde 3-phosphate dehydrogenase; IgG: immunoglobulin G [Color figure can be viewed at wileyonlinelibrary.com]

differentiation whereas both miR-139 overexpression and c-Fos knockdown significantly reduced CM-induced osteoclast differentiation despite presence of 27-HC (Figure 4c).

4 | DISCUSSION

The present study provides evidence to support the role of 27-HC on osteoclastogenesis in lung adenocarcinoma microenvironment. Previous studies have suggested that lung adenocarcinoma A549 cells can induce RANKL-independent osteoclast differentiation through secretion of IL-8 (Bendre et al., 2005). CM from breast cancer can also promote osteoclast differentiation by regulating microRNA expression (Ell et al., 2013). Considering that macrophages are recruited into tumor microenvironment during lung adenocarcinoma bone metastases (Lavin et al., 2017), we first investigated the effect of CM from coculture system of lung adenocarcinoma cells and THP-1-derived macrophages on osteoclast differentiation from RAW264.7 cells. After exposure of RAW264.7 cells to CM, the expression of miR-139 was inhibited and c-Fos expression was increased, which was enhanced by 27-HC treatment. Our previous result indicates that miR-139 overexpression impairs RANKL-induced osteoclast differentiation (Zhang et al., 2017), suggesting that CM might facilitate osteoclast differentiation from RAW264.7. As expected,

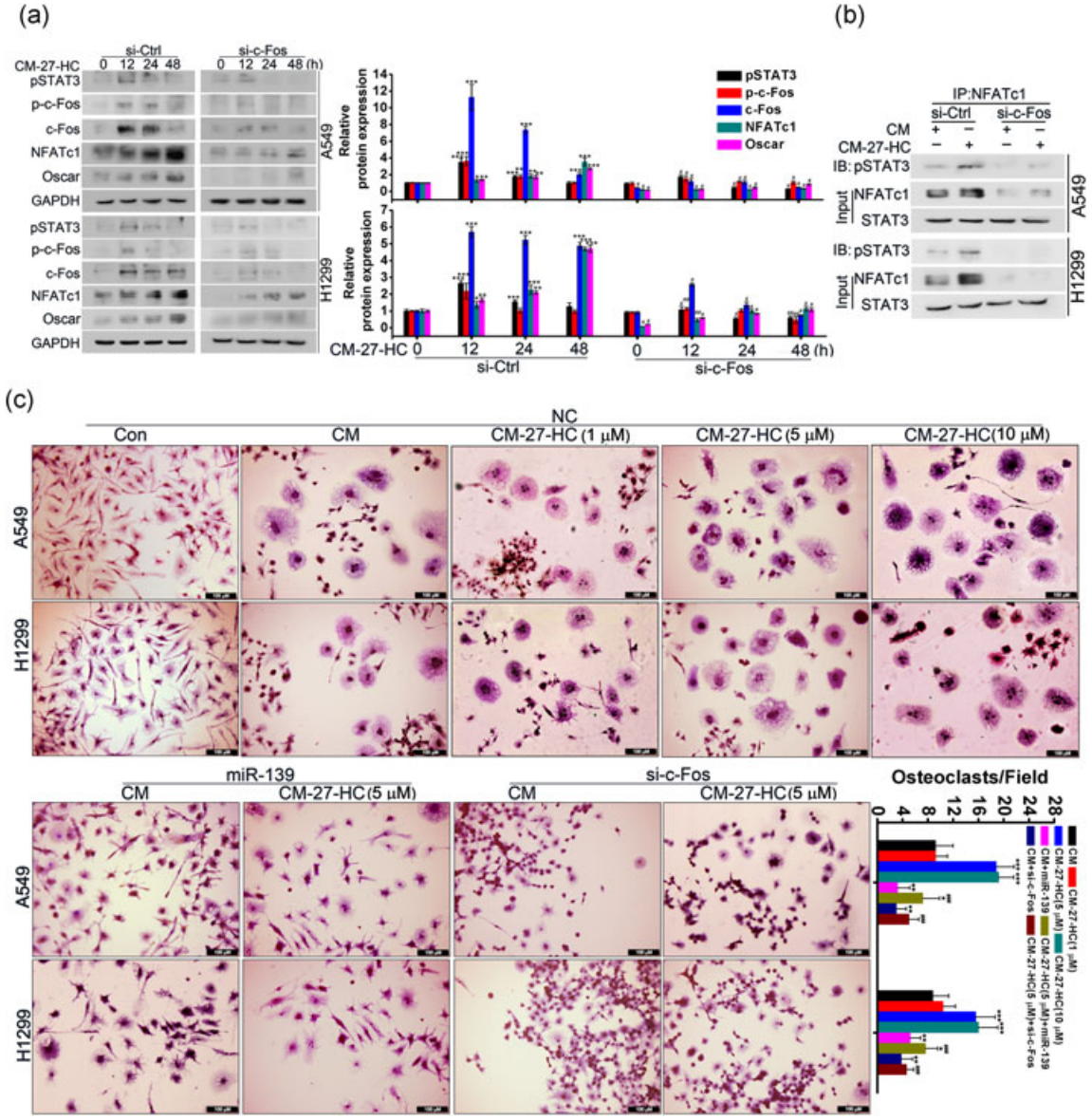

FIGURE 4 Knockdown of c-Fos inhibited-osteoclast differentiation. The RAW264.7 cells were transfected with negative control (NC) or siRNA against c-Fos, and were cultured for 2 days in CM containing 5 μM 27-HC. (a) The expression of pSTAT3, p-c-Fos, c-Fos, and NFATc1 were determined by western blot analysis. (b) The interaction between pSTAT3 and NFATc1 was determined by coimmunoprecipitation assay. (c) The RAW264.7 cells were transfected with NC, miR-139 or siRNA against c-Fos, and were cultured for 6 days in CM with or without the indicated concentration of 27-HC. Osteoclasts differentiation was measured by TRAP staining. Results are representative of at least three independent experiments. $^{*}p < 0.05$, $^{**}p < 0.01$, $^{***}p < 0.001$, $^{\#}p < 0.001$ versus the corresponding si-Ctrl group; $^{\#\#}p < 0.01$ versus the corresponding si-Ctrl group. 27-HC: 27-hydroxycholesterol; CM: conditioned media; GAPDH: glyceraldehyde 3-phosphate dehydrogenase; siRNA: small interfering RNA; TRAP: tartrate-resistant acid phosphatase [Color figure can be viewed at wileyonlinelibrary.com]

CM promoted osteoclast differentiation, especially in the presence of 27-HC. These results suggested that cytokines from CM could induce osteoclast differentiation, which was enlarged by 27-HC. 27-HC has been found to stimulate the release of several cytokines, such as TNF-α, CCL2 and IL-8 (S. M. Kim et al., 2013; Koarai et al., 2012; Lavin et al., 2017), among of which TNF-α and IL-8 have been demonstrated as stimulator of osteoclastogenesis (Bendre et al., 2005; Courbon et al., 2017). Thus, it was likely that 27-HC enhanced the secretion of these soluble factors to promote osteoclast differentiation via inhibition of miR-139.

The transcription factor c-Fos plays an important role in osteoclast differentiation. Mice lacking c-Fos gene develops into a severe osteopetrosis phenotype due to the impaired osteoclast differentiation (Johnson, Spiegelman, & Papaioannou, 1992). Furthermore, c-Fos regulates RANKL-induced NFATc1 expression that is a master control of osteoclast differentiation (M. Asagiri & Takayanagi, 2007). In this study, we found that c-Fos is a direct target of miR-139. It has been confirmed that miR-139 is implicated in hepatocellular carcinoma metastasis and inflammatory response by suppressing c-Fos expression (Fan et al., 2013;

Katsumi et al., 2016). Thus, it was reasonable that CM could increase c-Fos expression in RAW264.7 cells by inhibiting miR-139 expression.

We next tested the effect of CM in the absence or presence of 27-HC on NFATc1 expression. The results showed that exposure of RAW264.7 cells to CM promoted-NFATc1 expression, which was enhanced by 27-HC treatment. However, overexpression of miR-139 attenuated CM-induced NFATc1 expression despite in the presence of 27-HC. CM containing 27-HC also promoted the phosphorylation of STAT3, which was restrained by miR-139 overexpression. Overexpression of miR-139 blocked 27-HC-induced nuclear translocation of NFATc1. Overexpression of miR-139 has been demonstrated to inhibit the activity of calcineurin that activates the nuclear translocation of NFATc1 (M. Asagiri et al., 2005; Huang et al., 2010; Karieb & Fox, 2011; Xu et al., 2018), which might explain the inhibitory effect of miR-139 on the nuclear translocation of NFATc1. In addition, CM promoted the interaction between phosphorylated STAT3 and -NFATc1, which was enhanced by 27-HC. Overexpression of miR-139 significantly interfered with the communication between phosphorylated STAT3 and NFATc1, regardless of the presence of 27-HC, which should attribute to the suppressive effect of miR-139 on c-Fos expression. Knockdown of c-Fos similarly suppressed CM-induced STAT3 phosphorylation and NFATc1 expression despite the presence of 27-HC. NFATc1 acts as a master transcription factor that directly regulates the expression of osteoclast-related genes, such as Oscar. Our results suggested that both NFATc1 and pSTAT3 positively regulated Oscar expression. Mice deficient in c-Fos gene lost the ability of osteoclastogenesis, resulting in osteopetrosis (Johnson et al., 1992). However, ectopic expression of NFATc1 in c-Fos-deficient cells regained the capacity of osteoclast formation (Asagiri et al., 2005). Our results showed that CM-induced c-Fos expression before NFATc1 expression, and c-Fos could bind to the promoter of NFATc1, suggesting that NFATc1 is a downstream gene of c-Fos. Previous findings have revealed that overexpression of c-Fos can initiate RANKL-independent osteoclast differentiation (Jules et al., 2018). These results indicated that c-Fos upregulation induces osteoclast differentiation by directly increasing NFATc1 expression.

5 | CONCLUSION

In summary, 27-HC stimulated the secretion of some soluble factors from the CM of lung adenocarcinoma cells cocultured with THP-1-derived macrophages. CM promoted c-Fos expression in RAW264.7 cells by inhibiting miR-139 expression, which was enhanced by 27-HC. CM induced c-Fos-induced NFATc1 expression and STAT3 phosphorylation. 27-HC treatment further increased NFATc1 expression and STAT3 phosphorylation, which was blocked by miR-139 overexpression. Moreover, 27-HC facilitated nuclear translocation of NFATc1 and interaction between NFATc1 and phosphorylated STAT3, which was also suppressed by miR-139. C-Fos silencing mimicked the function of miR-139. These results suggested that 27-HC enhanced CM-induced osteoclastogenesis by regulating the miR-139/c-Fos pathway.

ACKNOWLEDGMENTS

This study was supported by the National Natural Science Foundation of China (Grant No. 81572272; 81201778), the Medical and Health Technology Development Plan Project of Shandong Province (Grant No. 2016WSB01041) and the Science and Technology Development Plan Project of Shandong Province (Grant No. 2015 GSF118083).

CONFLICTS OF INTEREST

The authors declare that there are no conflicts of interest.

ORCID

Yanliang Lin http://orcid.org/0000-0002-1682-3373

REFERENCES

Asagiri, M., Sato, K., Usami, T., Ochi, S., Nishina, H., Yoshida, H., … Takayanagi, H. (2005). Autoamplification of NFATc1 expression determines its essential role in bone homeostasis. *The Journal of Experimental Medicine*, *202*(9), 1261–1269.

Asagiri, M., & Takayanagi, H. (2007). The molecular understanding of osteoclast differentiation. *Bone*, *40*(2), 251–264.

Bendre, M. S., Margulies, A. G., Walser, B., Akel, N. S., Bhattacharrya, S., Skinner, R. A., … Suva, L. J. (2005). Tumor-derived interleukin-8 stimulates osteolysis independent of the receptor activator of nuclear factor-kappaB ligand pathway. *Cancer Research*, *65*(23), 11001–11009.

Bussard, K. M., Gay, C. V., & Mastro, A. M. (2008). The bone microenvironment in metastasis; what is special about bone? *Cancer Metastasis Reviews*, *27*(1), 41–55.

Carpenter, K. L. H., Taylor, S. E., van der Veen, C., Williamson, B. K., Ballantine, J. A., & Mitchinson, M. J. (1995). Lipids and oxidised lipids in human atherosclerotic lesions at different stages of development. *Biochimica et Biophysica Acta*, *1256*(2), 141–150.

Coughlin, T. R., Romero-Moreno, R., Mason, D. E., Nystrom, L., Boerckel, J. D., Niebur, G., & Littlepage, L. E. (2017). Bone: A fertile soil for cancer metastasis. *Current Drug Targets*, *18*(11), 1281–1295.

Courbon, G., Flammier, S., Laroche, N., Vico, L., Marotte, H., & Coury, F. (2017). Tumor necrosis factor alpha overexpression induces mainly osteoclastogenesis at the vertebral site. *Calcified Tissue International*, *100*(6), 575–584.

Ell, B., Mercatali, L., Ibrahim, T., Campbell, N., Schwarzenbach, H., Pantel, K., … Kang, Y. (2013). Tumor-induced osteoclast miRNA changes as regulators and biomarkers of osteolytic bone metastasis. *Cancer Cell*, *24*(4), 542–556.

Fan, Q., He, M., Deng, X., Wu, W. K. K., Zhao, L., Tang, J., … Liu, Y. (2013). Derepression of c-Fos caused by microRNA-139 down-regulation contributes to the metastasis of human hepatocellular carcinoma. *Cell Biochemistry and Function*, *31*(4), 319–324.

Hernández, I., Moreno, J. L., Zandueta, C., Montuenga, L., & Lecanda, F. (2010). Novel alternatively spliced ADAM8 isoforms contribute to the aggressive bone metastatic phenotype of lung cancer. *Oncogene*, *29*(26), 3758–3769.

Huang, H., Chikazu, D., Voznesensky, O. S., Herschman, H. R., Kream, B. E., Drissi, H., & Pilbeam, C. C. (2010). Parathyroid hormone induction of cyclooxygenase-2 in murine osteoblasts: Role of the calcium-calcineurin-NFAT pathway. *Journal of Bone and Mineral Research*, *25*(4), 819–829.

Hyeon, S., Lee, H., Yang, Y., & Jeong, W. (2013). Nrf2 deficiency induces oxidative stress and promotes RANKL-induced osteoclast differentiation. *Free Radical Biology and Medicine*, *65*, 789–799.

Johnson, R. S., Spiegelman, B. M., & Papaioannou, V. (1992). Pleiotropic effects of a null mutation in the c-fos proto-oncogene. *Cell*, *71*(4), 577–586.

Jules, J., Chen, W., Feng, X., & Li, Y. P. (2018). C/EBPalpha transcription factor is regulated by the RANK cytoplasmic (535)IVVY(538) motif and stimulates osteoclastogenesis more strongly than c-Fos. *The Journal of Biological Chemistry*, *293*(4), 1480–1492.

Karieb, S., & Fox, S. W. (2011). Phytoestrogens directly inhibit TNF-alpha-induced bone resorption in RAW264.7 cells by suppressing c-fos-induced NFATc1 expression. *Journal of Cellular Biochemistry*, *112*(2), 476–487.

Katsumi, T., Ninomiya, M., Nishina, T., Mizuno, K., Tomita, K., Haga, H., … Ueno, Y. (2016). MiR-139-5p is associated with inflammatory regulation through c-FOS suppression, and contributes to the progression of primary biliary cholangitis. *Laboratory Investigation*, *96*(11), 1165–1177.

Kim, S. M., Jang, H., Son, Y., Lee, S. A., Bae, S. S., Park, Y. C., … Kim, K. (2013). 27-hydroxycholesterol induces production of tumor necrosis factor-alpha from macrophages. *Biochemical and Biophysical Research Communications*, *430*(2), 454–459.

Kim, S. M., Lee, S. A., Kim, B. Y., Bae, S. S., Eo, S. K., & Kim, K. (2013). 27-hydroxycholesterol induces recruitment of monocytic cells by enhancing CCL2 production. *Biochemical and Biophysical Research Communications*, *442*(3-4), 159–164.

Koarai, A., Yanagisawa, S., Sugiura, H., Ichikawa, T., Kikuchi, T., Furukawa, K., … Ichinose, M. (2012). 25-hydroxycholesterol enhances cytokine release and toll-like receptor 3 response in airway epithelial cells. *Respiratory Research*, *13*, 63.

Koga, T., Matsui, Y., Asagiri, M., Kodama, T., de Crombrugghe, B., Nakashima, K., & Takayanagi, H. (2005). NFAT and Osterix cooperatively regulate bone formation. *Nature Medicine*, *11*(8), 880–885.

Kuo, P. L., Liao, S. H., Hung, J. Y., Huang, M. S., & Hsu, Y. L. (2013). MicroRNA-33a functions as a bone metastasis suppressor in lung cancer by targeting parathyroid hormone related protein. *Biochimica et Biophysica Acta*, *1830*(6), 3756–3766.

Lavin, Y., Kobayashi, S., Leader, A., Amir, E. D., Elefant, N., Bigenwald, C., … Merad, M. (2017). Innate immune landscape in early lung adenocarcinoma by paired single-cell analyses. *Cell*, *169*(4), 750–765 e717

Luis-Ravelo, D., Antón, I., Zandueta, C., Valencia, K., Ormazábal, C., Martínez-Canarias, S., … Lecanda, F. (2014). A gene signature of bone metastatic colonization sensitizes for tumor-induced osteolysis and predicts survival in lung cancer. *Oncogene*, *33*(43), 5090–5099.

Ma, J., Fu, G., Wu, J., Han, S., Zhang, L., Yang, M., … Wang, Y. (2016). 4-cholesten-3-one suppresses lung adenocarcinoma metastasis by regulating translocation of HMGB1, HIF1alpha and caveolin-1. *Cell Death and Disease*, *7*(9), e2372.

Park, B. K., Zhang, H., Zeng, Q., Dai, J., Keller, E. T., Giordano, T., … Wang, C. Y. (2007). NF-kappaB in breast cancer cells promotes osteolytic bone metastasis by inducing osteoclastogenesis via GM-CSF. *Nature Medicine*, *13*(1), 62–69.

Park, S. Y., Lee, S. W., Kim, H. Y., Lee, S. Y., Lee, W. S., Hong, K. W., & Kim, C. D. (2015). Suppression of RANKL-induced osteoclast differentiation by cilostazol via SIRT1-induced RANK inhibition. *Biochimica et Biophysica Acta*, *1852*, 2137–2144.

Pereira, M., Petretto, E., Gordon, S., Bassett, J. H. D., Williams, G. R., & Behmoaras, J. (2018). Common signalling pathways in macrophage and osteoclast multinucleation. *Journal of Cell Science*, *131*(11), jcs216267.

Schulze, J., Weber, K., Baranowsky, A., Streichert, T., Lange, T., Spiro, A. S., … Schinke, T. (2012). p65-Dependent production of interleukin-1beta by osteolytic prostate cancer cells causes an induction of chemokine expression in osteoblasts. *Cancer Letters*, *317*(1), 106–113.

Shih, L. Y., Shih, H. N., & Chen, T. H. (2004). Bone resorption activity of osteolytic metastatic lung and breast cancers. *Journal of Orthopaedic Research*, *22*(6), 1161–1167.

Thomas, R. J., Guise, T. A., Yin, J. J., Elliott, J., Horwood, N. J., Martin, T. J., & Gillespie, M. T. (1999). Breast cancer cells interact with osteoblasts to support osteoclast formation. *Endocrinology*, *140*(10), 4451–4458.

Wythe, S. E., Nicolaidou, V., & Horwood, N. J. (2014). Cells of the immune system orchestrate changes in bone cell function. *Calcified Tissue International*, *94*(1), 98–111.

Xu, M., Chen, X., Huang, Z., Chen, D., Yu, B., Chen, H., … Luo, Y. (2018). MicroRNA-139-5p suppresses myosin heavy chain I and IIa expression via inhibition of the calcineurin/NFAT signaling pathway. *Biochemical and Biophysical Research Communications*, *500*(4), 930–936.

Yamada, C., Aikawa, T., Okuno, E., Miyagawa, K., Amano, K., Takahata, S., … Kogo, M. (2016). TGF-beta in jaw tumor fluids induces RANKL expression in stromal fibroblasts. *International Journal of Oncology*, *49*(2), 499–508.

Zhang, L., Lv, Y., Xian, G., & Lin, Y. (2017). 25-hydroxycholesterol promotes RANKL-induced osteoclastogenesis through coordinating NFATc1 and Sp1 complex in the transcription of miR-139-5p. *Biochemical and Biophysical Research Communications*, *485*(4), 736–741.

SUPPORTING INFORMATION

Additional supporting information may be found online in the Supporting Information section at the end of the article.

How to cite this article: Zhang L, Liu M, Liu J, et al. 27-Hydroxycholesterol enhanced osteoclastogenesis in lung adenocarcinoma microenvironment. *J Cell Physiol*. 2018;1–9. https://doi.org/10.1002/jcp.27883